Tetrahedron 64 (2008) 5061–5071

Contents lists available at ScienceDirect

Tetrahedron

journal homepage: www.elsevier.com/locate/tet

# Unusual cycloartane glycosides from *Astragalus eremophilus*

Angela Perrone [a], Milena Masullo [a], Carla Bassarello [a], Elena Bloise [a], Arafa Hamed [b], Patrizia Nigro [a], Cosimo Pizza [a], Sonia Piacente [a,*]

[a] *Dipartimento di Scienze Farmaceutiche, Università degli Studi di Salerno, via Ponte Don Melillo, 84084 Fisciano (SA), Italy*
[b] *Faculty of Science, South Valley University, 81528 Aswan, Egypt*

ARTICLE INFO

*Article history:*
Received 18 December 2007
Received in revised form 5 March 2008
Accepted 19 March 2008
Available online 22 March 2008

*Keywords:*
*Astragalus eremophilus*
Cycloartane glycosides
Cytotoxic activity
NMR

ABSTRACT

Eleven new cycloartane-type glycosides, named eremophilosides A–K have been isolated from the aerial parts of *Astragalus eremophilus*. Their structures were elucidated by MS and NMR experiments and the relative configurational analysis of eremophilosides C and D was carried out on the basis of the recently reported *J*-based method. Additionally, the cytotoxic activity of these compounds in MCF7 and U937 cell lines was evaluated. All tested compounds, except eremophilosides B, C, and J were found to inhibit slightly the growth (controlling the cell cycle) and/or to induce death processes in U937 cell line, the most susceptible cell line. Eremophilosides A and K resulted the most effective to induce cell death, the first by necrosis while the latter by apoptosis.



## 1. Introduction

*Astragalus* L., the largest genus in the family Leguminosae, comprises 2000 species distributed mainly in the northern temperate regions and tropical African mountains and in particular it is represented by 32 species indigenous to Egypt.[1,2]

The roots of various *Astragalus* species represent very old and well-known drugs in traditional medicine for the treatment of nephritis, diabetes, leukemia, uterine cancer and as antiperspirant, diuretic, and tonic.[3] *Astragalus* species showed interesting pharmacological properties including hepatoprotective, immunostimulant, and antiviral activities.[4,5] Anti-inflammatory, analgesic, sedative, and cardiovascular activities are also reported.[4,6]

*Astragalus* species are known to be rich in two major classes of biologically active compounds, polysaccharides and saponins.[3] *Astragalus* polysaccharides are reported to have anticancer and immunostimulating effects.[4] The latter group of constituents is the most widely studied secondary metabolites: previous study on *Astragalus* saponins have reported the presence of cycloartane- and oleanene-type glycosides, which were found to exert biological activities.[4,5] The immunostimulant effects of several cycloartane glycosides on macrophage activation and expression of inflammatory cytokines were investigated.[7–9] Recently, cycloartanes from *Astragalus* species have attracted interest because of their leishmanicidal[10] and antibacterial activities.[7]

Phytochemical studies on several Egyptian *Astragalus* species have resulted in the isolation of a series of cycloartane-type saponins.[11–20] Some of these glycosides have shown interesting antitumor activity against human tumor cell lines and also AIDS antiviral activity,[18] others have been reported to act as modulators of lymphocyte proliferation.[15,16]

Cycloartane glycosides have been reported for their cytotoxic activity on several cancer lines including solid tumor (HepG2), blood tumor (HL-60), and drug resistant tumor (R-HepG2).[21] Moreover cancer chemopreventive effects of natural and semisynthetic cycloartane-type and related triterpenoids have been reported.[22]

On the basis of interesting activities reported for many *Astragalus* species and for cycloartane glycosides and as a part of our ongoing research of new bioactive compounds from Egyptian species, we have investigated the aerial parts of *Astragalus eremophilus* Boiss. (Leguminosae). This paper reports the isolation of eleven new cycloartane-type glycosides, named eremophilosides A–K (**1**–**11**). Their structures were elucidated by extensive spectroscopic methods including 1D- ($^{1}$H, $^{13}$C, and TOCSY) and 2D-NMR (DQF-COSY, HSQC, HMBC, HETLOC, and ROESY) experiments as well as ESIMS analysis.

Since cycloartane glycosides have shown to possess cytotoxic activity,[22] we have evaluated the potential effect of compounds **1**–**11** on tumor cell growth in MCF7 (breast carcinoma) and U937 (monocytic leukemia) cell lines.

* Corresponding author. Tel.: +39 089 969763; fax: +39 089 969602.
*E-mail address:* piacente@unisa.it (S. Piacente).

0040-4020/$ – see front matter © 2008 Elsevier Ltd. All rights reserved.
doi:10.1016/j.tet.2008.03.069

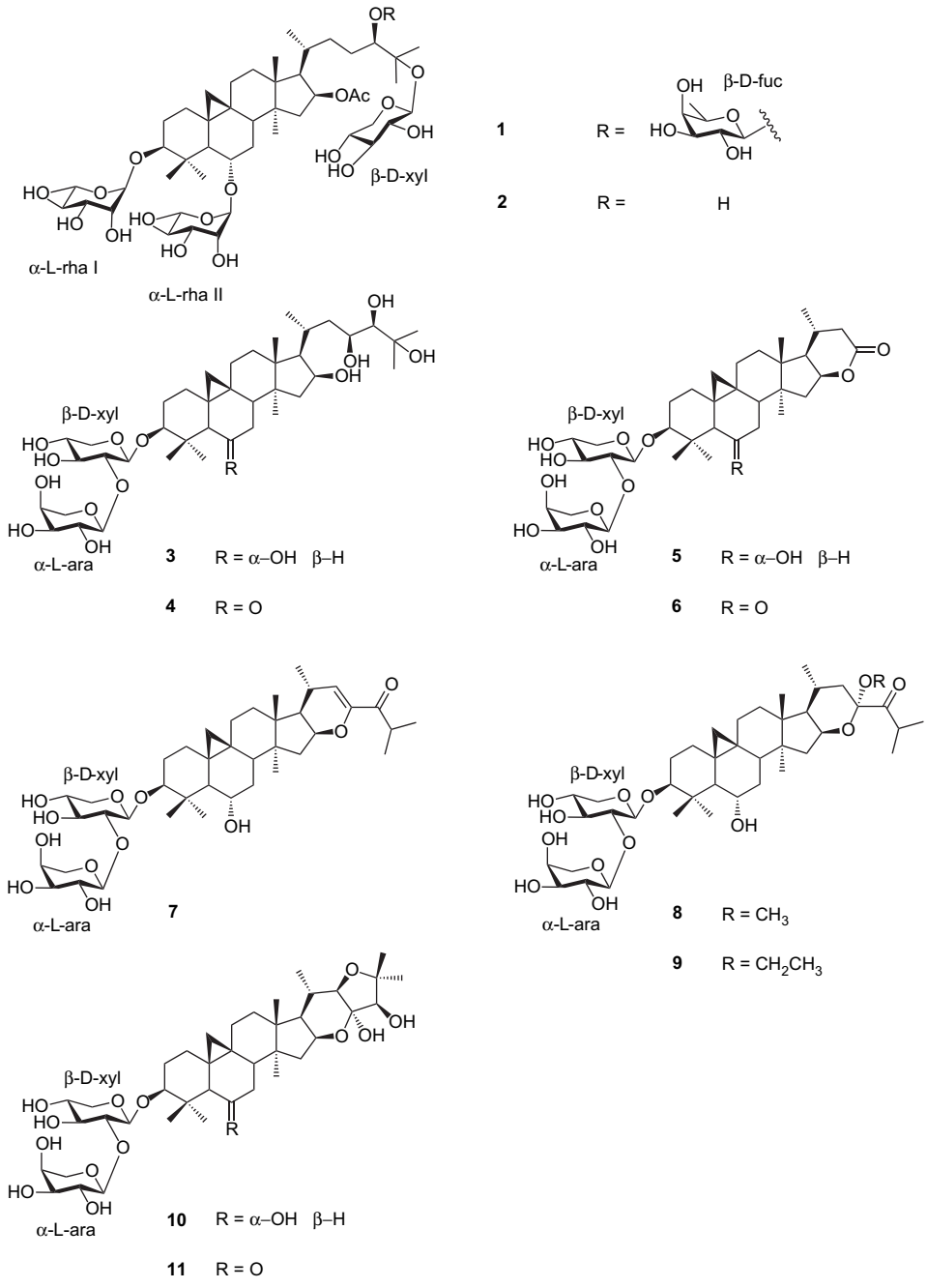


## 2. Results and discussion

### 2.1. Structural elucidation

The aerial parts of *A. eremophilus* were extracted with 70% EtOH and the obtained extract was fractionated over Sephadex LH-20. The fractions containing cycloartane glycosides were chromatographed by RP-HPLC and silica gel MPLC followed by RP-HPLC to yield 11 new compounds, **1**–**11** (see Section 4, Tables 1–5).

#### *2.1.1. Compound **1***

The HRMALDITOF mass spectrum of **1** showed a major ion peak at *m*/*z* 1127.5967 $[M+Na]^+$ ascribable to molecular formula $C_{55}H_{92}O_{22}$ (calcd for $C_{55}H_{92}O_{22}Na$, 1127.5978). The positive ESIMS spectrum of **1** gave the highest mass ion peak at *m*/*z* 1127 $[M+Na]^+$ and significant fragments in MS/MS analysis at *m*/*z* 1067 $[M+Na-60]^+$, due to the loss of an acetate molecule, at *m*/*z* 935 $[M+Na-60-132]^+$ and 921 $[M+Na-60-146]^+$, ascribable to the loss of a pentose and a 6-deoxyhexose unit, respectively. The $^1H$ NMR spectrum displayed for the sugar region signals corresponding to four anomeric protons at $\delta$ 4.76 (1H, d, $J$=1.2 Hz), 4.74 (1H, d, $J$=1.2 Hz), 4.62 (1H, d, $J$=7.6 Hz), and 4.47 (1H, d, $J$=7.5 Hz) (Table 1). The chemical shifts of all the individual protons of the four sugar units were ascertained from a combination of 1D-TOCSY and DQF-COSY spectral analysis, and the $^{13}C$ NMR chemical shifts of their attached carbons could be assigned unambiguously from the HSQC spectrum (see Table 1). These data showed the presence of two α-rhamnopyranosyl units ($\delta$ 4.76 and 4.74), one β-fucopyranosyl unit ($\delta$ 4.62) and one β-xylopyranosyl unit ($\delta$ 4.47). The $^1H$ NMR spectrum (Table 2) showed signals typical of cyclopropane methylene at

**Table 1**
$^{13}C$ and $^{1}H$ NMR data (*J* in Hz) of the sugar portions of compounds **1** and **3**–**11** ($CD_3OD$, 600 MHz)

| | **1** | | **3**[a] | |
|---|---|---|---|---|
| | α-L-RhaI | | β-D-Xyl | |
| 1 | 104.0 | 4.74, d (1.2) | 105.1 | 4.48, d (7.5) |
| 2 | 72.0 | 3.88, dd (1.2, 3.2) | 83.1 | 3.46, dd (9.2, 7.5) |
| 3 | 72.3 | 3.68, dd (3.2, 9.3) | 76.6 | 3.55, t (9.2) |
| 4 | 73.0 | 3.41, t (9.3) | 70.7 | 3.54, m |
| 5 | 69.8 | 3.72, m | 65.8 | 3.88, dd (11.7, 5.2) |
| | | | | 3.22, t (11.7) |
| 6 | 17.6 | 1.25, d (6.0) | | |
| | α-L-RhaII | | α-L-Ara | |
| 1 | 103.9 | 4.76, d (1.2) | 106.2 | 4.50, d (3.7) |
| 2 | 72.4 | 3.85, dd (1.2, 3.2) | 73.2 | 3.69, dd (8.5, 3.7) |
| 3 | 72.2 | 3.63, dd (3.2, 9.3) | 73.8 | 3.59, dd (8.5, 3.0) |
| 4 | 73.5 | 3.42, t (9.3) | 69.2 | 3.82, m |
| 5 | 69.5 | 3.70, m | 66.8 | 3.91, dd (11.9, 2.0) |
| | | | | 3.55, dd (11.9, 3.0) |
| 6 | 17.6 | 1.25, d (6.0) | | |
| | β-D-Fuc | | | |
| 1 | 104.9 | 4.62, d (7.6) | | |
| 2 | 73.3 | 3.41, dd (7.6, 8.5) | | |
| 3 | 75.7 | 3.41, dd (8.5, 2.5) | | |
| 4 | 73.7 | 3.56, m | | |
| 5 | 71.2 | 3.61, m | | |
| 6 | 16.4 | 1.30, d (6.5) | | |
| | β-D-Xyl | | | |
| 1 | 98.7 | 4.47, d (7.5) | | |
| 2 | 74.8 | 3.17, dd (9.2, 7.5) | | |
| 3 | 77.4 | 3.35, t (9.2) | | |
| 4 | 71.0 | 3.49, m | | |
| 5 | 66.4 | 3.82, dd (11.7, 5.2) | | |
| | | 3.22, t (11.7) | | |

[a] Being the same disaccharide chain, the chemical shift values of compounds **4**–**11** deviate from the experimental values of compound **3** of ±0.02 ppm.

δ 0.58 and 0.43 (each 1H, d, *J*=4.2 Hz), six tertiary methyl groups at δ 1.31, 1.22, 1.20, 1.11, 1.02, and 1.00, a secondary methyl group at δ 0.97 (d, *J*=6.5 Hz), and a signal at δ 2.10 (3H, s) ascribable to an acetoxy group. Additionally, four methine proton signals at δ 5.38 (ddd, *J*=8.0, 8.0, 5.2 Hz), 3.44 (ddd, *J*=9.5, 9.5, 4.5 Hz), 3.41 (dd, *J*=10.3, 2.2 Hz), 3.19 (dd, *J*=11.3, 4.0 Hz) were indicative of secondary alcoholic functions. The NMR data of the aglycon moiety of **1** were in good agreement with those of cycloasgenin C,[23] except for the downfield shifts of C-16 resonances ($\delta_H$ 5.38, $\delta_C$ 76.8), suggesting esterification at this position. The HMBC correlation between the proton signal at δ 5.38 (H-16) and the carbon resonance at δ 173.2 ($COCH_3$) confirmed the location of an acetoxy function at C-16. Full assignment of the $^{1}H$ and $^{13}C$ signals of the aglycon moiety of **1** showed glycosidation shifts for C-3 (δ 89.7), C-6 (δ 80.6), C-24 (86.8), and C-25 (83.4) (Table 5). These data, in combination with the absence of any $^{13}C$ glycosidation shifts for the four sugar units, suggested that **1** was an unusual tetradesmosidic saponin. This evidence was confirmed by the HMBC spectrum, which allowed us to establish the linkage sites of sugar units. Key correlation peaks between the proton signal at δ 4.76 ($H\text{-}1_{rhaII}$) and the carbon resonance at δ 80.6 (C-6), δ 4.74 ($H\text{-}1_{rhaI}$), and δ 89.7 (C-3), δ 4.62 ($H\text{-}1_{fuc}$) and δ 86.8 (C-24) and the proton signal at δ 4.47 ($H\text{-}1_{xyl}$) and the carbon resonance at δ 83.4 (C-25) were observed. Tetradesmosidic cycloartane glycosides are very unusual and to the author's knowledge only one tetradesmosidic cycloartane glycoside with an acyclic side chain, named cyclostipuloside E, was isolated from *Tragacantha stipulosa* (Leguminosae). Cyclostipuloside E was characterized by the same aglycon of **1** but with different sugar units and different glycosidation sites.[24] Thus the structure of **1** was established as the new 3-*O*-α-L-rhamnopyranosyl-6-*O*-α-L-rhamnopyranosyl-24-*O*-β-D-fucopyranosyl-25-*O*-β-D-xylopyranosyl-16-*O*-acetoxy-3β,6α,16β,24(*R*),25-pentahydroxycycloartane, named eremophiloside A.

**Table 2**
$^{1}H$ NMR data (*J* in Hz) of the aglycon moieties of compounds **1**, **3** and **4** (600 MHz, $CD_3OD$)

| Position | **1** | **3** | **4** |
|---|---|---|---|
| 1 | 1.63, 1.30, m | 1.57, 1.25, m | 1.76, 1.48, m |
| 2 | 1.97, 1.74, m | 1.95, 1.71, m | 1.98, 1.73, m |
| 3 | 3.19, dd (11.3, 4.0) | 3.23, dd (11.3, 4.0) | 3.23, dd (11.3, 4.0) |
| 4 | — | — | — |
| 5 | 1.60, d (9.5) | 1.39, d (9.5) | 2.39, s |
| 6 | 3.44, ddd (9.5, 9.5, 4.5) | 3.48, ddd (9.5, 9.5, 4.5) | — |
| 7 | 1.83, 1.44, m | 1.50, 1.39, m | 2.24, dd (12.0, 8.3) |
| | | | 2.20, dd (12.0, 3.6) |
| 8 | 1.83, m | 1.84, dd (11.9, 4.2) | 2.70, dd (8.3, 3.6) |
| 9 | — | — | — |
| 10 | — | — | — |
| 11 | 2.02, 1.30, m | 2.02, 1.23, m | 1.93, 1.60, m |
| 12 | 1.72 (2H), m | 1.69 (2H), m | 1.67, 1.61, m |
| 13 | — | — | — |
| 14 | — | — | — |
| 15 | 2.15, dd (12.7, 8.0) | 2.05, dd (12.7, 8.0) | 1.94, dd (12.7, 8.0) |
| | 1.35, dd (12.7, 5.2) | 1.43, dd (12.7, 5.2) | 1.42, dd (12.7, 5.2) |
| 16 | 5.38, ddd | 4.50, ddd | 4.52, ddd |
| | (8.0, 8.0, 5.2) | (8.0, 8.0, 5.2) | (8.0, 8.0, 5.2) |
| 17 | 1.93, dd (9.9, 8.0) | 1.78, dd (9.9, 8.0) | 1.80, dd (9.9, 8.0) |
| 18 | 1.20, s | 1.22, s | 1.18, s |
| 19 | 0.58, d (4.2) | 0.56, d (4.2) | 0.76, d (5.2) |
| | 0.43, d (4.2) | 0.40, d (4.2) | 0.27, d (5.2) |
| 20 | 1.75, m | 2.09, m | 2.12, m |
| 21 | 0.97, d (6.5) | 1.06, d (6.5) | 1.06, d (6.5) |
| 22 | 1.98, 0.78, m | 1.66 (2H), m | 1.64 (2H), m |
| 23 | 1.80, 1.07, m | 3.71, dd (8.5, 4.6) | 3.71, dd (8.5, 4.6) |
| 24 | 3.41, dd (10.3, 2.2) | 3.11, d (8.5) | 3.11, d (8.5) |
| 25 | — | — | — |
| 26 | 1.31, s | 1.27, s | 1.26, s |
| 27 | 1.22, s | 1.26, s | 1.25, s |
| 28 | 1.11, s | 1.32, s | 1.33, s |
| 29 | 1.00, s | 1.04, s | 1.06, s |
| 30 | 1.02, s | 1.00, s | 0.94, s |
| $-OCOCH_3$ | 2.10, s | — | — |

**Table 3**
$^{1}H$ NMR data (*J* in Hz) of the aglycon moieties of compounds **5**–**7** (600 MHz, $CD_3OD$)

| Position | **5** | **6** | **7** |
|---|---|---|---|
| 1 | 1.58, 1.27, m | 1.78, 1.49, m | 1.58, 1.27, m |
| 2 | 1.95, 1.70, m | 1.99, 1.75, m | 1.95, 1.71, m |
| 3 | 3.24, dd (11.3, 4.0) | 3.23, dd (11.3, 4.0) | 3.22, dd (11.3, 4.0) |
| 4 | — | — | — |
| 5 | 1.41, d (9.5) | 2.39, s | 1.40, d (9.5) |
| 6 | 3.51, ddd (9.5, 9.5, 4.5) | — | 3.50, ddd (9.5, 9.5, 4.5) |
| 7 | 1.54, 1.40, m | 2.31, dd (12.0, 8.3) | 1.53, 1.42, m |
| | | 2.22, dd (12.0, 3.6) | |
| 8 | 1.92, dd (11.9, 4.2) | 2.80, dd (8.3, 3.6) | 1.90, dd (11.9, 4.2) |
| 9 | — | — | — |
| 10 | — | — | — |
| 11 | 2.04, 1.34, m | 1.94, 1.63, m | 2.06, 1.30, m |
| 12 | 1.73, 1.60, m | 1.74, 1.49, m | 1.59 (2H), m |
| 13 | — | — | — |
| 14 | — | — | — |
| 15 | 2.12, dd (12.7, 8.0) | 2.04, dd (12.7, 8.0) | 2.16, dd (12.7, 8.0) |
| | 1.68, dd (12.7, 5.2) | 1.68, dd (12.7, 5.2) | 1.80, dd (12.7, 5.2) |
| 16 | 4.88, ddd (8.0, 8.0, 5.2) | 4.89, ddd (8.0, 8.0, 5.2) | 4.34, ddd (8.0, 8.0, 5.2) |
| 17 | 2.14, dd (9.9, 8.0) | 2.18, dd (9.9, 8.0) | 2.00, dd (9.9, 8.0) |
| 18 | 1.15, s | 1.10, s | 1.01, s |
| 19 | 0.62, d (4.2) | 0.82, d (5.2) | 0.60, d (4.2) |
| | 0.40, d (4.2) | 0.30, d (5.2) | 0.38, d (4.2) |
| 20 | 2.03, m | 2.03, m | 2.24, dd (9.9, 3.6) |
| 21 | 1.12, d (6.5) | 1.14, d (6.5) | 1.21, d (6.5) |
| 22 | 2.34 (2H), d (3.4) | 2.34 (2H), d (3.4) | 6.12, d (3.6) |
| 23 | — | — | — |
| 24 | — | — | — |
| 25 | — | — | 3.27, m |
| 26 | — | — | 1.08, d (6.7) |
| 27 | — | — | 1.07, d (6.7) |
| 28 | 1.32, s | 1.34, s | 1.33, s |
| 29 | 1.04, s | 1.06, s | 1.03, s |
| 30 | 1.06, s | 1.00, s | 1.06, s |

**Table 4**
$^1$H NMR data ($J$ in Hz) of the aglycon moieties of compounds **8**–**11** (600 MHz, $CD_3OD$)

| Position | **8** | **9** | **10** | **11** |
|---|---|---|---|---|
| 1 | 1.58, 1.27, m | 1.59, 1.30, m | 1.58, 1.26, m | 1.78, 1.48, m |
| 2 | 1.95, 1.71, m | 1.95, 1.71, m | 1.95, 1.71, m | 1.98, 1.73, m |
| 3 | 3.24, dd (11.3, 4.0) | 3.24, dd (11.3, 4.0) | 3.23, dd (11.3, 4.0) | 3.22, dd (11.3, 4.0) |
| 4 | — | — | — | — |
| 5 | 1.40, d (9.5) | 1.40, d (9.5) | 1.38, d (9.5) | 2.39, s |
| 6 | 3.50, ddd (9.5, 9.5, 4.5) | 3.50, ddd (9.5, 9.5, 4.5) | 3.48, ddd (9.5, 9.5, 4.5) | — |
| 7 | 1.54, 1.41, m | 1.54, 1.40, m | 1.50, 1.38, m | 2.23 (2H), m |
| 8 | 1.88, dd (11.9, 4.2) | 1.88, dd (11.9, 4.2) | 1.83, dd (11.9, 4.2) | 2.72, dd (8.3, 3.6) |
| 9 | — | — | — | — |
| 10 | — | — | — | — |
| 11 | 2.05, 1.30, m | 2.05, 1.31, m | 2.06, 1.27, m | 1.93, 1.62, m |
| 12 | 1.71, 1.63, m | 1.71, 1.63, m | 1.72, 1.65, m | 1.72, 1.50, m |
| 13 | — | — | — | — |
| 14 | — | — | — | — |
| 15 | 2.00, dd (12.7, 8.0) | 1.98, 1.59, Overlapped | 1.86, dd (12.7, 8.0) | 1.77, dd (12.7, 8.0) |
| | 1.60, dd (12.7, 5.2) | | 1.47, dd (12.7, 5.2) | 1.46, dd (12.7, 5.2) |
| 16 | 4.35, ddd (8.0, 8.0, 5.2) | 4.37, ddd (8.0, 8.0, 5.2) | 4.54, ddd (8.0, 8.0, 5.2) | 4.55, ddd (8.0, 8.0, 5.2) |
| 17 | 1.68, dd (9.9, 8.0) | 1.69, dd (9.9, 8.0) | 1.56, dd (9.9, 8.0) | 1.61, dd (9.9, 8.0) |
| 18 | 1.18, s | 1.18, s | 1.17, s | 1.13, s |
| 19 | 0.60, d (4.2) | 0.60, d (4.2) | 0.58, d (4.2) | 0.78, d (5.2) |
| | 0.41, d (4.2) | 0.40, d (4.2) | 0.41, d (4.2) | 0.30, d (5.2) |
| 20 | 1.58, m | 1.56, m | 1.57, m | 1.61, m |
| 21 | 0.96, d (6.5) | 0.96, d (6.5) | 1.02, d (6.5) | 1.03, d (6.5) |
| 22 | 1.97, 1.36, m | 1.98, 1.38, m | 3.35, d (10.6) | 3.35, d (10.6) |
| 23 | — | — | — | — |
| 24 | — | — | 3.67, s | 3.68, s |
| 25 | 3.28, m | 3.28, m | — | — |
| 26 | 1.11, d (6.7) | 1.10, d (6.7) | 1.27, s | 1.27, s |
| 27 | 1.08, d (6.7) | 1.08, d (6.7) | 1.21, s | 1.22, s |
| 28 | 1.32, s | 1.33, s | 1.33, s | 1.32, s |
| 29 | 1.05, s | 1.05, s | 1.04, s | 1.06, s |
| 30 | 1.02, s | 1.03, s | 1.00, s | 0.96, s |
| $-OCH_3$ | 3.13, s | — | — | — |
| $-OCH_2CH_3$ | — | 3.47, 3.22, m | — | — |
| $-OCH_2CH_3$ | — | 1.16, t (7.1) | — | — |

*2.1.2. Compound **2***

The molecular formula of **2** was established to be $C_{49}H_{82}O_{18}$ by HRMALDITOFMS analysis ($m/z$ 981.5401 $[M+Na]^+$, calcd for $C_{49}H_{82}O_{18}Na$, 981.5399). The positive ESIMS spectrum showed the major ion peak at $m/z$ 981 $[M+Na]^+$. Its MS/MS fragmentation showed peaks at $m/z$ 921 $[M+Na-60]^+$, 789 $[M+Na-60-132]^+$, 775 $[M+Na-60-146]^+$, similar to compound **1**. The $^1$H NMR and $^{13}$C chemical shifts of the aglycon moiety were almost superimposable on those of **1** except for C-24 ($\delta_H$ 3.32 and $\delta_C$ 78.9), C-25 ($\delta$ 80.9), Me-26 ($\delta_H$ 1.23 and $\delta_C$ 21.0), and Me-27 ($\delta_H$ 1.23 and $\delta_C$ 23.3) resonances. Additionally for the sugar portion of **2** in comparison with that of **1**, signals only for three anomeric protons were observed in the $^1$H NMR spectrum at $\delta$ 4.77 (1H, d, $J$=1.2 Hz), 4.73 (1H, d, $J$=1.2 Hz), and 4.48 (1H, d, $J$=7.5 Hz). These data, in combination with 1D-TOCSY, HSQC, HMBC, DQF-COSY correlations, showed that **2** differed from **1** only by the absence of a β-fucopyranosyl unit at C-24. Therefore, compound **2** was identified as the new 3-*O*-α-L-rhamnopyranosyl-6-*O*-α-L-rhamnopyranosyl-*O*-β-D-xylopyranosyl-16-*O*-acetoxy-3β,6α,16β,24(*R*),25-pentahydroxycycloartane, named eremophiloside B.

*2.1.3. Compounds **3**–**11***

A detailed comparison of the sugar region NMR data ($^1$H, $^{13}$C, 1D-TOCSY, HSQC, HMBC, DQF-COSY) and ESIMS data of compounds **3**–**11** showed that the disaccharide chain was identical in the nine compounds. In particular for the sugar portion, compound **3** showed in the $^1$H NMR spectrum signals corresponding to two anomeric protons at $\delta$ 4.48 (1H, d, $J$=7.5 Hz) and 4.50 (1H, d, $J$=3.7 Hz) (Table 1). Complete assignments of the $^1$H and $^{13}$C NMR signals of the sugar portion were accomplished by 1D-TOCSY, HSQC, HMBC, and DQF-COSY experiments, which led to the identification of one β-xylopyranosyl unit ($\delta$ 4.48) and one α-arabinopyranosyl unit ($\delta$ 4.50). The determination of the sequence and linkage sites was obtained from the HMBC correlations between the proton signals at $\delta$ 4.48 (H-$1_{xyl}$) and the carbon resonance at $\delta$ 89.4 (C-3), and the proton signal at $\delta$ 4.50 (H-$1_{ara}$) and the carbon resonance at $\delta$ 83.1 (C-$2_{xyl}$). Thus, the sugar sequence of compounds **3**–**11** was established as 3-*O*-α-L-arabinopyranosyl-(1→2)-β-D-xylopyranoside.

The HRMALDITOF mass spectrum of **3** ($m/z$ 795.4504 $[M+Na]^+$, calcd for $C_{40}H_{68}O_{14}Na$, 795.4507) supported a molecular formula of $C_{40}H_{68}O_{14}$. The ESIMS mass spectrum showed the major ion peak at $m/z$ 795, which was assigned to $[M+Na]^+$. The MS/MS of this ion showed peaks at $m/z$ 663 $[M+Na-132]^+$, corresponding to the loss of an arabinopyranosyl unit, at $m/z$ 513 $[M+Na-132-132]^+$, ascribable to the loss of a xylopyranosyl unit and at $m/z$ 305 $[M+Na-490]^+$, due to the loss of the aglycon moiety.

As concerning the aglycon moiety, the $^1$H NMR spectrum (Table 2) showed signals due to a cyclopropane methylene at $\delta$ 0.56 and 0.40 (each 1H, d, $J$=4.2 Hz), six tertiary methyl groups at $\delta$ 1.32, 1.27, 1.26, 1.22, 1.04, and 1.00, a secondary methyl group at $\delta$ 1.06 (d, $J$=6.5 Hz), and five methine proton signals at $\delta$ 4.50 (ddd, $J$=8.0, 8.0, 5.2 Hz), 3.71 (dd, $J$=8.5, 4.6 Hz), 3.48 (ddd, $J$=9.5, 9.5, 4.5 Hz), 3.23 (dd, $J$=11.3, 4.0 Hz), and 3.11 (d, $J$=8.5 Hz), which were indicative of secondary alcoholic functions. It was also evident that the singlet signal at $\delta$ 2.10 ascribable to the further methyl group of the acetyl residue in **2** was absent in **3**. On this basis, comparison of the aglycon region HSQC and HMBC spectra of compound **3** with those of compound **2** revealed that the aglycon of compound **3** differs from that of **2** by the lack of the acetyl function on C-16, and by the presence of an additional hydroxyl group on C-23. Then, the complete $^1$H and $^{13}$C chemical shift assignments for **3** were determined using the conventional combination of 2D-NMR experiments. Final inspection of $^1$H and $^{13}$C NMR spectra indicated compound **3** to be a member of the cycloorbygenin C class of compounds.

**Table 5**
$^{13}$C NMR data of the aglycon moieties of compounds **1** and **3**–**11** (600 MHz, $CD_3OD$)

| Position | 1 | 3 | 4 | 5 | 6 | 7 | 8 | 9 | 10 | 11 |
|---|---|---|---|---|---|---|---|---|---|---|
| 1 | 32.5 | 33.0 | 31.2 | 33.0 | 31.1 | 33.1 | 32.9 | 33.2 | 33.1 | 31.1 |
| 2 | 29.5 | 30.2 | 29.4 | 30.3 | 29.4 | 30.4 | 30.2 | 30.2 | 30.4 | 29.5 |
| 3 | 89.7 | 89.4 | 89.4 | 89.5 | 88.4 | 89.6 | 89.4 | 89.4 | 89.4 | 88.7 |
| 4 | 42.6 | 42.9 | 42.2 | 42.8 | 41.8 | 43.2 | 43.0 | 42.8 | 42.7 | 41.8 |
| 5 | 53.0 | 54.6 | 58.8 | 54.4 | 58.8 | 54.7 | 54.4 | 54.4 | 54.5 | 58.8 |
| 6 | 80.6 | 69.1 | 214.6 | 68.8 | 215.0 | 69.3 | 69.0 | 68.9 | 69.1 | 215.0 |
| 7 | 34.8 | 38.6 | 42.2 | 38.3 | 42.0 | 38.8 | 38.5 | 38.6 | 38.7 | 42.4 |
| 8 | 47.5 | 48.5 | 44.1 | 47.8 | 43.5 | 48.8 | 47.9 | 48.0 | 48.2 | 44.3 |
| 9 | 21.4 | 21.7 | 22.4 | 21.8 | 22.4 | 22.0 | 21.8 | 21.9 | 21.3 | 22.4 |
| 10 | 29.4 | 29.9 | 30.5 | 30.6 | 30.9 | 30.5 | 30.4 | 30.3 | 29.8 | 30.9 |
| 11 | 26.6 | 26.6 | 27.0 | 26.6 | 26.9 | 26.8 | 26.6 | 26.7 | 26.6 | 27.2 |
| 12 | 33.2 | 33.4 | 33.4 | 33.1 | 32.6 | 30.8 | 33.6 | 33.8 | 34.1 | 34.0 |
| 13 | 46.4 | 46.5 | 46.4 | 45.6 | 45.8 | 46.6 | 45.5 | 45.4 | 45.3 | 45.8 |
| 14 | 47.8 | 47.8 | 48.2 | 47.2 | 48.3 | 47.9 | 47.6 | 47.3 | 47.2 | 48.3 |
| 15 | 46.1 | 47.9 | 45.3 | 44.4 | 42.1 | 46.8 | 43.8 | 44.1 | 43.7 | 41.7 |
| 16 | 76.8 | 73.0 | 72.7 | 82.3 | 81.6 | 77.0 | 73.5 | 73.6 | 72.8 | 72.6 |
| 17 | 56.8 | 58.2 | 57.2 | 55.2 | 54.3 | 53.1 | 57.2 | 57.4 | 52.5 | 52.0 |
| 18 | 18.3 | 18.3 | 15.4 | 20.3 | 17.9 | 19.1 | 20.7 | 20.7 | 20.6 | 17.8 |
| 19 | 30.2 | 31.2 | 22.3 | 31.0 | 21.9 | 32.2 | 31.2 | 31.5 | 31.9 | 22.6 |
| 20 | 32.0 | 27.4 | 27.8 | 28.0 | 27.7 | 25.5 | 26.5 | 26.5 | 36.5 | 36.5 |
| 21 | 18.2 | 19.9 | 19.9 | 21.3 | 21.8 | 25.1 | 20.5 | 20.5 | 16.8 | 17.2 |
| 22 | 34.4 | 42.6 | 42.8 | 39.0 | 38.6 | 118.5 | 39.9 | 40.3 | 85.4 | 85.3 |
| 23 | 30.2 | 72.8 | 72.8 | 177.1 | 177.3 | 150.3 | 104.3 | 104.0 | 103.5 | 103.3 |
| 24 | 86.8 | 79.3 | 79.4 | — | — | 203.6 | 215.7 | 215.4 | 81.9 | 82.0 |
| 25 | 83.4 | 74.5 | 74.5 | — | — | 35.5 | 36.0 | 36.0 | 80.8 | 80.6 |
| 26 | 19.5 | 23.7 | 23.8 | — | — | 18.8 | 19.2 | 19.2 | 28.8 | 29.1 |
| 27 | 24.3 | 28.0 | 27.7 | — | — | 18.9 | 19.3 | 19.3 | 21.1 | 21.4 |
| 28 | 28.9 | 28.3 | 26.7 | 28.2 | 26.7 | 28.6 | 28.2 | 28.4 | 28.3 | 26.8 |
| 29 | 16.4 | 16.0 | 14.9 | 15.9 | 15.0 | 16.1 | 15.8 | 16.0 | 15.9 | 15.1 |
| 30 | 20.2 | 20.1 | 19.2 | 19.6 | 18.6 | 21.2 | 19.7 | 19.7 | 19.7 | 18.9 |
| $-OCOCH_3$ | 173.2 | — | — | — | — | — | — | — | — | — |
| $-OCOCH_3$ | 21.8 | — | — | — | — | — | — | — | — | — |
| $-OCH_3$ | — | — | — | — | — | — | 51.0 | — | — | — |
| $-OCH_2CH_3$ | — | — | — | — | — | — | — | 59.6 | — | — |
| $-OCH_2CH_3$ | — | — | — | — | — | — | — | 15.6 | — | — |

Recently, the absolute configurations of C-23 and C-24 stereocenters in cycloorbicoside D were determined as *R* based on single-crystal X-ray diffraction.[25] In order to ascertain the absolute configurations of C-23 and C-24, it was first necessary to determine the relative configuration of such segment C-23–C-24. We pursued this goal by employing the *J*-based analysis,[26] and by using pyridine-$d_5$ as solvent system. The use of pyridine-$d_5$ left open the possibility that ROE couplings including the protons on oxygens could be used to substantiate the configurational assignments. Indeed, for segment C-23–C-24 the sole *J*-couplings accurately measured from a PFG-HETLOC spectrum in solvent system $CD_3OD$ ($^3J_{H\text{-}23\text{–}H\text{-}24}$=8.3 Hz, $^2J_{H\text{-}23\text{–}C\text{-}24}$=−2.8 Hz, $^2J_{H\text{-}24\text{–}C\text{-}23}$=−3.1 Hz, and $^3J_{H\text{-}24\text{–}C\text{-}22}$=2.5 Hz) were consistent with the two H-23 and H-24 *anti*-conformers with opposite relative configurations whereas, inspecting the ROESY spectrum, no key dipolar couplings were observed in $CD_3OD$ for a subsequent conclusive and safe differentiation between the two rotamers. Moreover, the diastereotopic methylene protons on C-22 that appeared practically identical in $CD_3OD$ could instead be distinguished in pyridine-$d_5$, thereby allowing us to relate H-23 to H-20 through the methylene protons on C-22 (Table 6).

For the relative configuration of C-23–C-24, the large homonuclear coupling of $^3J_{H\text{-}23\text{–}H\text{-}24}$ 8.5 Hz, together with the $^2J_{H\text{-}23\text{–}C\text{-}24}$ of −3.3 Hz, and the $^3J_{H\text{-}24\text{–}C\text{-}22}$ of 0.5 Hz, indicated an *anti* relationship between H-23 and H-24 protons, while the pattern of ROE effects observed in pyridine-$d_5$ between H-22b and 24-OH, between Me-26 and 23-OH, and Me-27and 23-OH gave decisive support to our assignment.

For the C-22–C-23 segment, because the proton NMR signals for H-22a, H-22b, and H-15 were partly overlapping multiplets, the relative configuration was deduced from the magnitude of the $^{2,3}J_{H,C}$ heteronuclear coupling constants in conjunction with observed ROE effects. The $^2J_{H\text{-}22a\text{–}C\text{-}23}$ of −4.3 Hz and the $^2J_{H\text{-}22b\text{–}C\text{-}23}$ of −1.7 Hz indicated that H-22a and H-22b were in a *gauche* and an *anti* relationship with respect to the 23-OH, respectively. Also, the small values of $^3J_{H\text{-}22a\text{–}C\text{-}24}$ and of $^3J_{H\text{-}22b\text{–}C\text{-}24}$ pointed to the rotamer depicted in Table 7. On this basis, we could assess that H-22a, appearing as a broad doublet doublet with *J*=13.4, 9.1 Hz and H-22b, appearing as a broad doublet of doublet with *J*=13.4, 7.7 Hz, were in an *anti* and in a *gauche* orientation to H-23, respectively. Furthermore, the above evidence allowed us to deduce a *gauche* and an *anti* orientation to H-20 for H-22a and H-22b, respectively. Finally, the pattern of the ROE cross-peaks suggested, with a high level of confidence, that the configuration of the C-20–C-22 segment was of the *syn*-type. In particular, the presence of a strong ROE effect between Me-21 and H-23, and of two weak ROE effects between H-17 and H-22a, and H-17 and H-22b were fully consistent with the configuration depicted in Table 7.

On this basis, the aglycon of **3** was identified as cycloorbigenin C[27] and for **3** was determined the new structure of 3-*O*-[α-L-arabinopyranosyl-(1→2)-β-D-xylopyranosyl]-3β,6α,16β,23(*R*),24(*R*),25-hexahydroxycycloartane, named eremophiloside C.

The HRMALDITOF mass spectrum of **4** showed a major ion peak at *m*/*z* 793.4354 $[M+Na]^+$ ascribable to molecular formula $C_{40}H_{66}O_{14}$ (calcd for $C_{40}H_{66}O_{14}Na$, 793.4350). The positive ESIMS mass spectrum gave the highest ion peak at *m*/*z* 793, which was assigned to $[M+Na]^+$. Also the MS/MS of this ion showed peaks at *m*/*z* 661 $[M+Na-132]^+$ and at *m*/*z* 511 $[M+Na-132-132]^+$, corresponding to the stepwise loss of the two sugar units, and at *m*/*z* 305 $[M+Na-488]^+$, due to the loss of the aglycon moiety. The $^1H$ and $^{13}C$ NMR data of **4** in comparison with those of **3** showed that the signals of C and D rings and side chain were in good agreement except for the upfield shifts of C-18 and C-19 (Table 5). Additionally, in the $^1H$ NMR spectrum of **4** the signals of H-5 (δ 2.39), $H_2$-7 (δ 2.24

**Table 6**
$^{13}C$ and $^{1}H$ NMR data ($J$ in Hz) of the aglycon moiety of compound **3** (Py-$d_5$, 600 MHz)

| Position | **3** | |
|---|---|---|
| 1 | 32.3 | 1.65, 1.26, m |
| 2 | 30.1 | 2.36, 2.02, m |
| 3 | 88.4 | 3.59, dd (11.0, 4.2) |
| 4 | 42.6 | — |
| 5 | 53.8 | 1.75, d (9.1) |
| 6 | 67.5 | 3.80, ddd (9.1, 9.1, 4.5) |
| 7 | 38.3 | 1.82, 1.67, m |
| 8 | 46.5 | 1.95, dd (11.2, 4.4) |
| 9 | 21.1 | — |
| 10 | 29.2 | — |
| 11 | 26.1 | 1.89, 1.21, m |
| 12 | 32.7 | 1.63 (2H), m |
| 13 | 45.6 | — |
| 14 | 46.6 | — |
| 15 | 47.6 | 2.15, dd (12.1, 7.3)<br>1.75, m |
| 16 | 71.9 | 4.71, q (7.1) |
| 17 | 57.3 | 1.84, dd (10.3, 8.0) |
| 18 | 18.6 | 1.37, s |
| 19 | 29.5 | 0.58, d (4.0)<br>0.27, d (4.0) |
| 20 | 27.1 | 2.58, m |
| 21 | 20.2 | 1.19, d (6.4) |
| 22b | 42.8 | 2.17 br dd (13.4, 7.7) |
| 22a | | 2.12, br dd (13.4, 9.1) |
| 23 | 72.9 | 4.32, br t (9.1, 8.5) |
| 24 | 78.9 | 3.75, dd (8.5, 5.8) |
| 25 | 74.2 | — |
| 26 | 24.5 | 1.71, s |
| 27 | 28.9 | 1.67, s |
| 28 | 28.6 | 1.98, s |
| 29 | 16.0 | 1.44, s |
| 30 | 19.9 | 1.01, s |
| 6-*OH* | — | 5.31, br s |
| 16-*OH* | — | 5.80, d (2.0) |
| 23-*OH* | — | 6.84, d (2.2) |
| 24-*OH* | — | 6.60, d (5.8) |
| 25-*OH* | — | 6.44, br s |

**Table 7**
Dominant rotamers of compound chain (**3**) C2-fragments along with their relative configurations (Py-$d_5$, 600 MHz)

| Fragment | Segment | $^{2,3}J$ (Hz) | ROE |
|---|---|---|---|
| C-20–C-22 *syn*-(20*S*,22a*S*,22b*R*) | 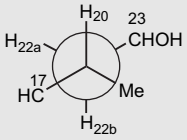 | $^{3}J_{H\text{-}20\text{–}H\text{-}22a}$ Small<br>$^{3}J_{H\text{-}20\text{–}H\text{-}22b}$ 7.7 | H-23–Me s<br>H-23–H-20 s<br>H-22a–H-20 m<br>H-22a–H-17 w<br>H-22b–H-17 w<br>H-22b–Me w |
| C-22–C-23 *anti*-(22a*S*,22b*R*,23*S*) | 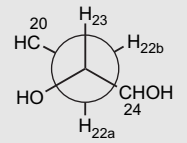 | $^{3}J_{H\text{-}23\text{–}H\text{-}22a}$ 9.1<br>$^{3}J_{H\text{-}23\text{–}H\text{-}22b}$ Small<br>$^{2}J_{H\text{-}22a\text{–}C\text{-}23}$ −4.7<br>$^{3}J_{H\text{-}22a\text{–}C\text{-}24}$ 0.8<br>$^{2}J_{H\text{-}22b\text{–}C\text{-}23}$ −1.7<br>$^{3}J_{H\text{-}22b\text{–}C\text{-}24}$ 1.0 | H-23–H-22b m<br>H-22b–H-24 w<br>H-22a–H-24 m<br>H-22a–23-OH w<br>H-20–23-OH m |
| C-23–C-24 *anti*-(23*S*, 24*S*) | 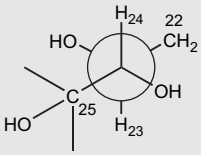 | $^{3}J_{H\text{-}23\text{–}H\text{-}24}$ 8.5<br>$^{2}J_{H\text{-}23\text{–}C\text{-}24}$ −3.3<br>$^{3}J_{H\text{-}24\text{–}C\text{-}22}$ 0.7 | H-22b–24-OH w<br>Me-26–23-OH w<br>Me-27–23-OH w |

The intensity of dipolar effects (ROESY) is expressed in terms of three categories: s=strong, m=medium, w=weak.

and $\delta$ 2.20), and H-8 ($\delta$ 2.70) were displaced downfield, while the H-6 signal was absent. Also shifts of signals due to cyclopropane methylene ($\delta$ 0.76 and $\delta$ 0.27) were observed (Table 2). These data allowed us to suggest the presence of a keto function in the A or B ring supported by the absorption peak in the IR spectrum at 1734 $cm^{-1}$ and by the presence of a signal at $\delta$ 214.6 in the $^{13}C$ NMR spectrum (Table 5). The HMBC spectrum displayed cross-peaks between the proton signals at $\delta$ 2.39 (H-5), 2.24 and 2.20 ($H_2$-7), $\delta$ 2.70 (H-8) and the keto function at $\delta$ 214.6, suggesting the location of keto function at C-6. Thus the structure of **4** was characterized as the new 3-*O*-[α-L-arabinopyranosyl-(1→2)-β-D-xylopyranosyl]-3β,16β,23(*R*),24(*R*),25-pentahydroxycycloartan-6-one, named eremophiloside D.

The HRMALDITOF mass spectrum of **5** showed a major ion peak at $m/z$ 703.3665 $[M+Na]^+$ ascribable to molecular formula $C_{36}H_{56}O_{12}$ (calcd for $C_{36}H_{56}O_{12}Na$, 703.3669). The positive ESIMS mass spectrum gave the highest ion peak at $m/z$ 703 $[M+Na]^+$. Its MS/MS fragmentation showed peaks at $m/z$ 571 $[M+Na-132]^+$, corresponding to the loss of an arabinopyranosyl unit, at $m/z$ 439 $[M+Na-132-132]^+$, ascribable to the loss of a xylopyranosyl unit, and at $m/z$ 305 $[M+Na-398]^+$, due to the loss of the aglycon moiety. The IR spectrum of **5** showed an absorption peak at 1740 $cm^{-1}$ due to a carbonyl group. For the aglycon portion in the $^{1}H$ NMR spectrum (Table 3) two characteristic cyclopropane methylenes at $\delta$ 0.62 and 0.40 (each 1H, d, $J$=4.2 Hz), four tertiary methyl groups at $\delta$ 1.32, 1.15, 1.06 and 1.04, a secondary methyl group at $\delta$ 1.12 (d, $J$=6.5 Hz), and three methine proton signals at $\delta$ 4.88 (ddd, $J$=8.0, 8.0, 5.2 Hz), 3.51 (ddd, $J$=9.5, 9.5, 4.5 Hz), 3.24 (dd, $J$=11.3, 4.0 Hz), indicative of secondary alcoholic functions, were observed. The NMR data of **5** in comparison to those of the aglycon of cimilactone A[28] revealed that compound **5** differed from cimilactone A only by the presence of a secondary alcoholic function to C-6 and for the absence of an acetoxy group at C-12. HBMC correlations between H-16 ($\delta$ 4.88), H-20 ($\delta$ 2.03) and H-22 ($\delta$ 2.34) and the carbonyl group at $\delta$ 177.1 confirmed the presence of a six-membered lactone ring between C-23 and C-16. On the basis of these data the aglycon of **5** was identified as a rare tetranor-cycloartane resulting from a loss of four carbons from C-24 to C-27 of a cycloartane with an acyclic side chain. Tetranor-cycloartane glycosides are very unusual in the plant kingdom and so far have only been isolated from the *Cimicifuga* species. Thus, the new structure 3-*O*-[α-L-arabinopyranosyl-(1→2)-β-D-xylopyranosyl]-3β,6α,16β-trihydroxy-24,25,26,27-tetranorcycloartan-23,16β-olide was assigned to eremophiloside E (**5**).

The molecular formula of **6** was determined to be $C_{36}H_{54}O_{12}$ by HRMALDITOFMS analysis ($m/z$ 701.3518 $[M+Na]^+$, calcd for $C_{36}H_{54}O_{12}Na$, 701.3513). The NMR data ($^{1}H$, $^{13}C$, DQF-COSY, HSQC, HMBC, ROESY) of **6** in comparison to those of **5** showed that **6** differed only by the presence of a keto function located at C-6. Therefore, compound **6** was established as the new 3-*O*-[α-L-arabinopyranosyl-(1→2)-β-D-xylopyranosyl]-3β,16β-dihydroxy-24,25,26,27-tetranorcycloartan-6-on-23,16β-olide, named eremophiloside F.

The HRMALDITOFMS analysis of compound **7** ($m/z$ 757.4132 $[M+Na]^+$, calcd for $C_{40}H_{62}O_{12}Na$, 757.4139) supported a molecular formula of $C_{40}H_{62}O_{12}$. The IR spectrum displayed carbonyl group at 1740 $cm^{-1}$. The $^{1}H$ NMR spectrum of the aglycon portion showed (Table 3) an olefinic proton at $\delta$ 6.12 (d, $J$=3.6 Hz), two cyclopropane methylenes at $\delta$ 0.60 and 0.38 (each 1H, d, $J$=4.2 Hz), four tertiary methyl groups at $\delta$ 1.33, 1.06, 1.03 and 1.01, three secondary methyl groups at $\delta$ 1.21 (d, $J$=6.5 Hz), 1.08 (d, $J$=6.7 Hz), and 1.07 (d, $J$=6.7 Hz), and three methine proton signals at $\delta$ 4.34 (ddd, $J$=8.0, 8.0, 5.2 Hz), 3.50 (ddd, $J$=9.5, 9.5, 4.5 Hz), 3.22 (dd, $J$=11.3, 4.0 Hz) indicative of secondary alcoholic functions. Furthermore, a multiplet proton signal at $\delta$ 3.27, in combination with the presence of two secondary methyls at $\delta$ 1.08 and 1.07, supported the existence of an isopropyl group in the aglycon. A detailed analysis of NMR data ($^{1}H$, $^{13}C$, DQF-COSY, HSQC, HMBC) suggested that **7** was a cycloartane triterpene with an α,β-unsaturated carbonyl group. In particular in the $^{13}C$ NMR spectrum (Table 5) appeared two unsaturated carbon signals at $\delta$ 118.5 and 150.3 and a carbonyl signal at $\delta$ 203.6. The

latter was assigned to a keto group at C-24 on the basis of HMBC correlations between the signals of protons of isopropyl group at $\delta$ 3.27 (H-25), 1.08 and 1.07 (H-26, 27) and the carbon resonance at $\delta$ 203.6. The HMBC spectrum showed also correlation peaks between the olefinic proton at $\delta$ 6.12 (H-22) and a methine carbon at $\delta$ 25.5 (C-20), a secondary methyl at $\delta$ 25.1 (C-21), and a keto function at $\delta$ 203.6 (C-24), consistent with an unusual double bond between C-22 and C-23 and in agreement with $^{13}$C NMR data reported for similar compounds.[29] The chemical shift value of C-24 at $\delta$ 203.6 can be justified by the presence of the double bond conjugated to the keto function. Moreover, the existence of an heterocycle six-membered ring may also explain the downfield shift at $\delta$ 203.6 of C-24. Therefore, the structure of **7** was elucidated as the new 3-*O*-[α-L-arabinopyranosyl-(1→2)-β-D-xylopyranosyl]-3β,6α-dihydroxy-16β,23-epoxy-22,23-didehydro-25-hydrocycloartan-24-one, named eremophiloside G. While cycloartane glycosides with similar modifications of side chain have been previously described,[29] this is the first time that a saponin with these structural features has been isolated from *Astragalus* genus.

The molecular formula of compounds **8** and **9** was unequivocally established to be $C_{41}H_{66}O_{13}$ and $C_{42}H_{68}O_{13}$ by HRMALDITOFMS analysis (*m*/*z* 789.4407 $[M+Na]^+$, calcd for $C_{41}H_{66}O_{13}Na$, 789.4401, and *m*/*z* 803.4563 $[M+Na]^+$ calcd for $C_{42}H_{68}O_{13}Na$, 803.4558), respectively. The NMR data ($^1$H, $^{13}$C, DQF-COSY, HSQC, HMBC, ROESY) of **8** in comparison to those of **7** revealed that compounds **8** differed from **7** only by the absence of the double bond between C-22 and C-23 and the presence of a methoxy group ($\delta_H$ 3.13, $\delta_C$ 51.0) of a ketalic function at C-23 ($\delta$ 104.3). The α orientation of the methoxy group at C-23 was deduced from the ROESY spectrum in which a diagnostic correlation between the signal of $OCH_3$ group and H-16 ($\delta$ 4.35) was observed. On the basis of NMR analysis compound **9** differed from **8** only by the replacement of the methoxy group with an ethoxy group ($\delta_H$ 3.47 and 3.22, $\delta_C$ 59.6, $OCH_2CH_3$; $\delta_H$ 1.16, $\delta_C$ 15.6, $OCH_2CH_3$) at C-23 ($\delta$ 104.3) (Tables 4 and 5). Thus, the structure of **8** was identified as 3-*O*-[α-L-arabinopyranosyl-(1→2)-β-D-xylopyranosyl]-3β,6α-dihydroxy-23α-methoxy-16β,23-epoxy-25-hydrocycloartan-24-one, named eremophiloside H, and the structure of **9** was characterized as 3-*O*-[α-L-arabinopyranosyl-(1→2)-β-D-xylopyranosyl]-3β,6α-dihydroxy-23α-ethoxy-16β,23-epoxy-25-hydrocycloartan-24-one, named eremophiloside I. Compounds **7**, **8**, and **9** can be considered as secondary products formed from a common hemiketal precursor that would give eremophiloside G (**7**) by elimination and eremophilosides H (**8**) and I (**9**) by transformation into 23-*O*-methoxy- and 23-*O*-ethoxy-ketalic derivatives.

The HRMALDITOF mass spectrum of **10** showed a major ion peak at *m*/*z* 791.4199 $[M+Na]^+$ ascribable to molecular formula $C_{40}H_{64}O_{14}$ (calcd for $C_{40}H_{64}O_{14}Na$, 791.4194). The positive ESIMS mass spectrum gave the highest ion peak at *m*/*z* 791 $[M+Na]^+$. Its MS/MS fragmentation showed peaks at *m*/*z* 659 $[M+Na-132]^+$, corresponding to the loss of an arabinopyranosyl unit, at *m*/*z* 527 $[M+Na-132-132]^+$, ascribable to the additional loss of a xylopyranosyl unit and at *m*/*z* 305 $[M+Na-486]^+$, due to the loss of the aglycon moiety. The $^1$H NMR spectrum for the aglycon moiety displayed cyclopropane methylene signals at $\delta$ 0.58 and 0.41 (each 1H, d, *J*=4.2 Hz), six tertiary methyl groups at $\delta$ 1.33, 1.27, 1.21, 1.17, 1.04 and 1.00, a secondary methyl group at $\delta$ 1.02 (d, *J*=6.5 Hz), and five methine proton signals at $\delta$ 4.54 (ddd, *J*=8.0, 8.0, 5.2 Hz), 3.67 (s), 3.48 (ddd, *J*=9.5, 9.5, 4.5 Hz), 3.35 (d, *J*=10.6 Hz), and 3.23 (dd, *J*=11.3, 4.0 Hz) indicative of secondary alcoholic functions. In the $^{13}$C NMR spectrum, besides glycosidic carbons, the remaining downfield signals were assigned to five oxymethine carbons ($\delta$ 89.4, 85.4, 81.9, 72.8, and 69.1) and two oxygenated quaternary carbons ($\delta$ 103.5 and 80.8), one of which was a hemiketal. All of the above evidence suggested that the aglycon of **10** was a highly oxygenated cycloartane triterpene. The 2D-NMR data (DQF-COSY, HMBC, HSQC, ROESY) of the aglycon of **10** were very similar to those of cimiacerogenin B,[30] except for the presence of an α-OH group at C-6 ($\delta_H$ 3.48, $\delta_C$ 69.1). Furthermore, the ROESY spectrum showed cross-peaks between H-16 ($\delta$ 4.54) and H-22 ($\delta$ 3.35) and $H_3$-30 ($\delta$ 1.00), and between H-22 and H-24 ($\delta$ 3.67), confirming the β-orientation of secondary alcoholic functions at C-16, C-22, and C-24. Therefore, compound **10** was characterized as the new 3-*O*-[α-L-arabinopyranosyl-(1→2)-β-D-xylopyranosyl]-3β,6α,23α,24β-tetrahydroxy-16β,23;22β,25-diepoxy-cycloartane, named eremophiloside J.

Compound **11** showed a highest ion peak at *m*/*z* 789.4043 $[M+Na]^+$ in the HRMALDITOF mass spectrum, supporting a molecular formula $C_{40}H_{62}O_{14}$ (calcd for $C_{40}H_{62}O_{14}Na$, 789.4037). On the basis of NMR data ($^1$H, $^{13}$C, DQF-COSY, HMBC, HSQC, ROESY) of **11** in comparison to those of **10**, the aglycon of **11** displayed a keto function at C-6 ($\delta$ 215.0) instead of a secondary alcoholic function. Thus the structure of eremophiloside K was established as the new 3-*O*-[α-L-arabinopyranosyl-(1→2)-β-D-xylopyranosyl]-3β,23α,24β-trihydroxy-16β,23;22β,25-diepoxy-cycloartan-6-one (**11**).

## 2.2. Cytotoxic activity

To evaluate the cytotoxic potential of compounds **1**–**11**, their effects on tumor cell growth in MCF7 (breast carcinoma) and U937 (monocytic leukemia) cell lines were investigated.

Cells of hematopoietic origin (U937) resulted more susceptible to growth inhibition effects than those derived from a solid tumor (MCF7).

Exponentially growing cultures of U937 and MCF7 cell lines were exposed to increasing concentrations (1–100 μM) of test compounds or to vehicle alone and the number of cells was evaluated at 48 h. All tested compounds, except compounds **2**, **3**, and **10**, were found to inhibit tumor cell growth in this range of doses. To compare the growth inhibition potency of tested compounds, results obtained at 50 μM of each compound are summarized in Figure 1. All compounds inhibited to a higher extent U937 than MCF7 cells. In particular, compounds **4**, **6**, and **9** became effective on MCF7 only at 100 μM (data not shown). Compounds **1**, **5**, and **8** were the most active on both cell lines.

Further experiments aimed to get a more insight into the mechanisms underlying growth inhibition potential of active compounds were performed on U937 cell line. In particular, we

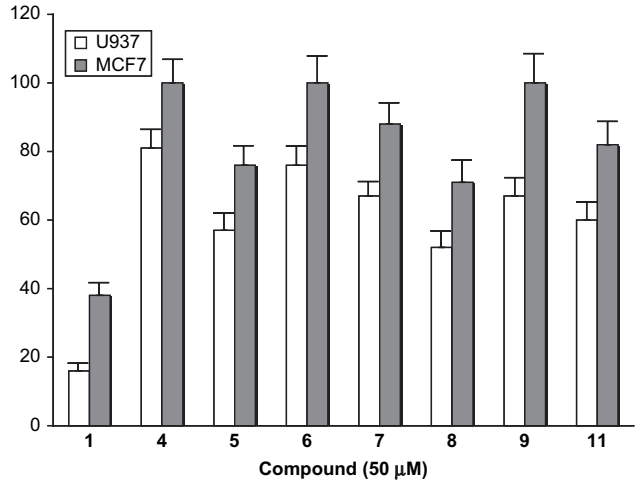


**Figure 1.** Cell growth inhibition by compounds **1**–**11**. U937 ($2\times10^4$/well) and MCF7 ($1\times10^4$/well) cells were cultured in the absence and in the presence of each compound (50 μM) or vehicle only (control) up to 48 h and the number of cells was determined as described in Section 4. Data are reported as the percentages of the number of control cells. Values represent the mean value±SD of two independent experiments performed in quintuplicate wells.

**Table 8**
Analysis of cell death induction in U937 cells by tested compounds[a]

| Compound | % Hypodiploid cells[b] | % Necrotic cells[b] |
|---|---|---|
| — | 1.23±0.09 | 1.60±0.10 |
| **1** | 21.96±4.6** | 79.00±5.1** |
| **4** | 1.67±0.10 | 1.34±0.05 |
| **5** | 4.23±0.23* | 1.87±0.88 |
| **6** | 2.54±0.12 | 2.31±0.10 |
| **7** | 6.17±0.22** | 2.43±0.14 |
| **8** | 7.62±0.26** | 3.48±0.18* |
| **9** | 2.72±0.09 | 1.74±0.06 |
| **11** | 9.18±0.16** | 4.13±0.11** |

*$P<0.05$, **$P<0.01$.
[a] Apoptosis and primary necrosis were measured in cells exposed to tested compounds (50 μM) for 24 h by flow cytometry as described in Experimental section. Control cells were treated with an equal volume of vehicle only. Results are expressed as the percentages of the total cell population analyzed (10,000 events).
[b] Values represent the mean value±SD of two separate experiments performed in triplicate.

analyzed whether the reduction of U937 cell number by test compounds was related mainly to the induction of cell death (cytotoxic effect) or cell cycle arrest (cytostatic effect). The cytotoxic activity (necrosis and/or apoptosis induction) of compounds and their effects on cell cycle distribution are summarized in Tables 8 and 9, respectively. Compound **1** displayed high cytotoxic potential, and activated mainly necrotic mode of cell death. Compounds **5**, **7**, **8**, and **11** induced a slight, but significant, increase of apoptotic cell death, whereas compounds **4**, **6**, and **9** failed almost completely to induce apoptotic or necrotic cell death. Thus, if the ability of compound **1** to induce cell death can account for the reduction of cell number by this compound, other mechanisms, such as cell cycle impairment, could be responsible or contribute to the growth inhibitory effect of the remaining compounds. Accordingly, both compounds **4**, **6**, **9** and compounds **5**, **7**, **8**, **11** were found to cause a delay in the cell cycle progression. In particular, most of them (**4**, **6**, **9**, **5**, **7**, **11**) caused cells to accumulate in the S phase of cell cycle with a concomitant reduction of the percentage of cells in G2/M. Compound **8**, like compound **1**, caused instead cells to accumulate the G0/G1 phase. Representative cell cycle profiles of control and compound **9** or **8** treated cells are reported in Figure 2.

All together the above data indicate that tested compounds, except compounds **2**, **3**, and **10**, are effective in reducing U937 cell growth, but they act through different mechanisms: (i) compound **1** through necrotic cell death induction, preceded by cell accumulation in G0/G1; (ii) compounds **5**, **7**, and **11** through both apoptosis and S arrest induction; (iii) compound **8** through both apoptosis and G0/G1 arrest induction; (iv) compounds **4**, **6**, and **9** only through the induction of cell block in S.

**Table 9**
Effects of tested compounds on cell cycle distribution[a]

| Compound | G0/G1 (% of cells)[b] | S phase (% of cells)[b] | G2/M (% of cells)[b] |
|---|---|---|---|
| — | 43.01±1.1 | 42.98±1.7 | 14.01±0.34 |
| **1** | 58.0±3.80 | 34.2±2.02 | 8.0±1.40 |
| **4** | 39.0±0.73 | 55.8±1.61 | 6.10±0.65 |
| **5** | 44. 7±1.90 | 54.9±2.30 | 1.61±0.7 |
| **6** | 40.1±2.16 | 58.0±2.60 | 2.30±0.1 |
| **7** | 43.4±1.91 | 53.2±2.94 | 4.09±0.7 |
| **8** | 54.6±1.72 | 46.1±1.71 | 0.13±0.1 |
| **9** | 32.9±2.50 | 64.3±2.62 | 0.70±0.03 |
| **11** | 43.0±0.91 | 50.4±2.21 | 6.61±1.6 |

[a] U937 cells were exposed to tested compounds (50 μM) or to an equivalent volume of vehicle for 24 h.
[b] Values represent the mean value±SD of two separate experiments performed in triplicate.

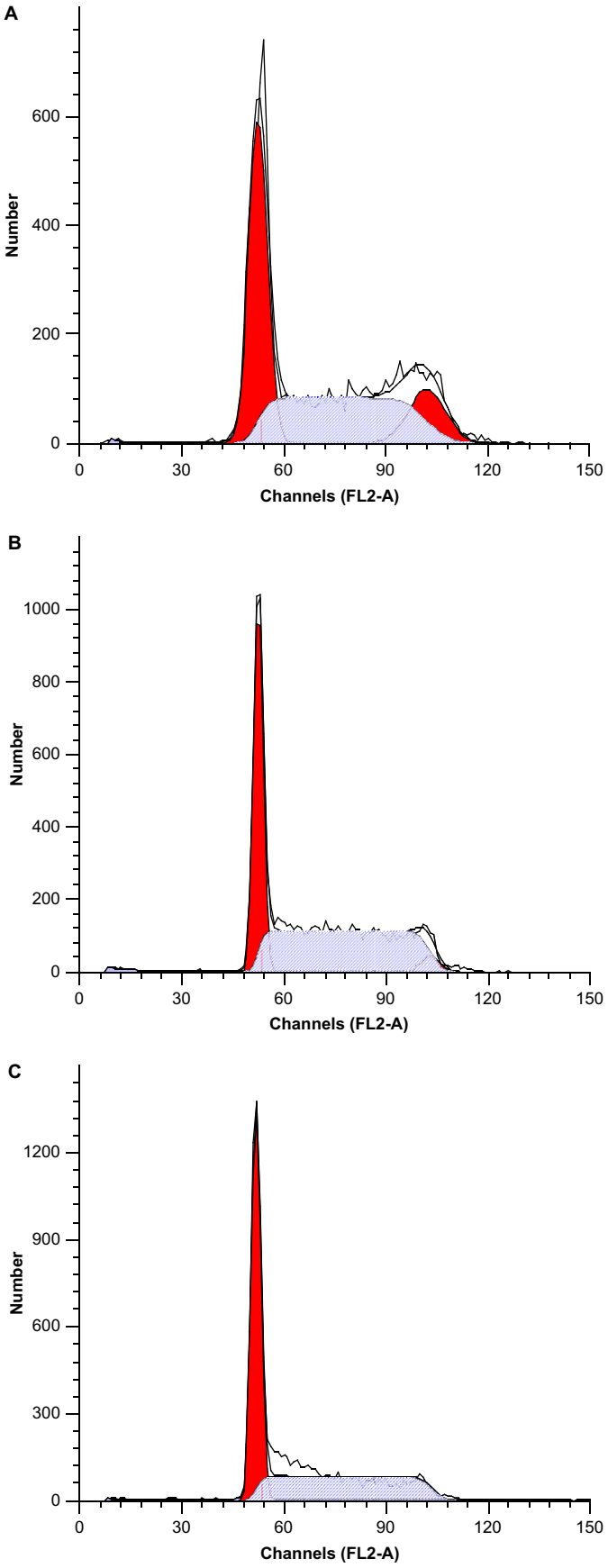


**Figure 2.** Representative histograms of cell cycle distribution of U937 cells treated with vehicle only (A), 50 μM compound **9** (B), or 50 μM compound **8** (C).

## 3. Conclusion

Eremophilosides A–K are characterized mainly by different structural features of the side chain: eremophilosides A–D (**1**–**4**) present an acyclic side chain, eremophilosides E–I (**5**–**9**) are 16β,23-epoxycycloartanes, while eremophilosides J (**10**) and K (**11**) are 16β,23;22β,25-diepoxycycloartanes. In particular, eremophiloside A (**1**) is the first report of a tetradesmosidic saponin with a cycloartane-type aglycon possessing an acyclic side chain isolated from *Astragalus* species.

Eremophilosides E (**5**) and F (**6**) are characterized by an unusual loss of four carbons of the side chain from C-24 to C-27 and by the presence of a six-membered lactone ring between C-23 and C-16, while eremophilosides G–I (**7**–**9**) show unusual modifications of the cyclic side chain reported for the first time in the genus *Astragalus*. Finally, eremophilosides J (**10**) and K (**11**) are highly oxygenated cycloartane triterpenes never reported until now in *Astragalus* species.

## 4. Experimental

### 4.1. General experimental procedures

Optical rotations were measured on a JASCO DIP 1000 polarimeter. IR measurements were obtained on a Bruker IFS-48 spectrometer. NMR experiments were performed on a Bruker DRX-600 spectrometer equipped with a Bruker 5 mm TCI CryoProbe at 300 K. All 2D-NMR spectra were acquired in $CD_3OD$ (99.95%, Sigma–Aldrich) and standard pulse sequences and phase cycling were used for DQF-COSY, HSQC, HMBC, and ROESY spectra. For **3** the relative configurational attribution has been performed by dissolving the sample in $CD_3OD$ ($^1H$, $\delta$=3.34 ppm; $^{13}C$, $\delta$=49.0 ppm), and in pyridine-$d_5$ (99.5%, Sigma–Aldrich) ($^1H$, $\delta$=8.71, 7.55, 7.19 ppm; $^{13}C$, $\delta$=149.9, 135.5, 123.5 ppm). Phase-sensitive PFG-HETLOC spectrum was acquired for compound **3** with a number of 32 scans/$t_1$, 4K points in $\omega_2$, a spin lock of 50 ms and a $t_{1max}$ value of 26.7 ms in $CD_3OD$, and with a number of 440 scans/$t_1$, 4K points in $\omega_2$, a spin lock of 50 ms and a $t_{1max}$ value of 37.6 ms in pyridine-$d_5$, respectively.[31] The ROESY spectra were acquired with $t_{mix}$=400 ms.

Exact masses were measured by a Voyager DE mass spectrometer. Samples were analyzed by matrix-assisted laser desorption ionization time-of-flight (MALDITOF) mass spectrometry. A mixture of analyte solution and α-cyano-4-hydroxycinnamic acid (Sigma) was applied to the metallic sample plate and dried. Mass calibration was performed with the ions from ACTH (fragment 18–39) at 2465.1989 Da and angiotensin III at 931.5154 Da as internal standard. ESIMS analyses were performed using a ThermoFinnigan LCQ Deca XP Max ion-trap mass spectrometer equipped with Xcalibur software. Column chromatography was performed over Sephadex LH-20 (Pharmacia), MPLC was carried out on a Büchi C-605 chromatography pump equipped with a pump manager Büchi C-615 and Büchi B-685 borosilicate glass column (230×26 mm). Silica gel 60 (0.040–0.063 mm; Carlo Erba) was used as column material. Semi-preparative RP-HPLC was performed on a Waters 590 system equipped with a Waters R401 refractive index detector, a Waters XTerra Prep $MSC_{18}$ column (300×7.8 mm i.d.) and a Rheodyne injector. TLC was performed on silica gel F254 (Merck) plates, and reagent grade chemicals (Carlo Erba) were used throughout.

### 4.2. Plant material

Fresh samples of *A. eremophilus* Boiss. aerial parts were collected at Hurghada (Red Sea, Egypt) in March 2004 and identified by Prof. M. G. Sheded. A voucher specimen (no. 11352) was deposited at the Botany Department Herbarium, Faculty of Science of Aswan, Egypt.

### 4.3. Extraction and isolation

The plant material (900 g) was extracted with 70% EtOH (3×1.5 L) for 20 days. The solvent was removed under reduced pressure to afford 57.9 g of crude extract. Part of the extract (2.5×3 g) was fractionated on Sephadex LH-20 (100×5 cm) using MeOH as the mobile phase. Seventy fractions (8 mL) were obtained. Fraction 14 (78.5 mg) was chromatographed by RP-HPLC using MeOH–$H_2O$ (7:3) as mobile phase (flow rate 2.5 mL/min) to yield compounds **2** (3.2 mg, $t_R$=20.0 min) and **1** (3.5 mg, $t_R$=33.0 min). The next fractions containing cycloartane glycosides (fractions 15–21, 920 mg) were chromatographed by MPLC on silica gel with a gradient (flow rate 15.0 mL/min) of $CHCl_3$–MeOH (from 100:0–85:15, stepwise) as eluent to afford 3120 fractions (8 mL) monitored by TLC. Fractions 328–404 (37.6 mg) were chromatographed by RP-HPLC using MeOH–$H_2O$ (4:1) as mobile phase (flow rate 2.5 mL/min) to yield compounds **11** (1.2 mg, $t_R$=10.1 min) and **6** (1.0 mg, $t_R$=16.8 min). Fractions 409–796 (44.6 mg) were chromatographed by RP-HPLC using MeOH–$H_2O$ (4:1) as mobile phase (flow rate 2.5 mL/min) to yield compounds **7** (1.2 mg, $t_R$=20.1 min), **8** (1.2 mg, $t_R$=26.1 min), and **9** (1.0 mg, $t_R$=34.7 min). Fractions 797–942 (20.7 mg) were chromatographed by RP-HPLC using MeOH–$H_2O$ (3:1) as mobile phase (flow rate 2.5 mL/min) to yield compound **5** (2.3 mg, $t_R$=8.4 min). Fractions 1405–1780 (34.6 mg) were chromatographed by RP-HPLC using MeOH–$H_2O$ (7:3) as mobile phase (flow rate 2.5 mL/min) to yield compounds **4** (1.0 mg, $t_R$=11.1 min) and **10** (1.1 mg, $t_R$=24.4 min). Fractions 1781–2728 (43.7 mg) were chromatographed by RP-HPLC using MeOH–$H_2O$ (3:2) as mobile phase (flow rate 2.5 mL/min) to yield compound **3** (4.2 mg, $t_R$=34.1 min).

#### 4.3.1. Eremophiloside A (*1*)

White amorphous powder; mp 264–266 °C; $[\alpha]_D^{25}$ +8.7 (*c* 0.2, MeOH); IR (KBr) $\nu_{max}$ 3420, 2933, 1735, 1250–1024 $cm^{-1}$; $^1H$ NMR ($CD_3OD$, 600 MHz) data of aglycon moiety, see Table 2; $^{13}C$ NMR ($CD_3OD$, 150 MHz) data of aglycon moiety, see Table 5; $^1H$ NMR ($CD_3OD$, 600 MHz) and $^{13}C$ NMR ($CD_3OD$, 150 MHz) data of sugar portion, see Table 1; ESIMS *m/z* 1127 $[M+Na]^+$; ESIMS/MS *m/z* 1067 $[M+Na-60]^+$, 935 $[M+Na-60-132]^+$, 921 $[M+Na-60-146]^+$; HRMALDITOFMS *m/z* 1127.5967 $[M+Na]^+$ (calcd for $C_{55}H_{92}O_{22}Na$, 1127.5978).

#### 4.3.2. Eremophiloside B (*2*)

White amorphous powder; mp 270–272 °C; $[\alpha]_D^{25}$ −2.5 (*c* 0.2, MeOH); IR (KBr) $\nu_{max}$ 3400, 2940, 1734, 1271–1050 $cm^{-1}$; $^1H$ NMR ($CD_3OD$, 600 MHz) data of aglycon moiety superimposable on those reported for compound **1**, excepted for H-24 ($\delta$ 3.32, dd, *J*=10.3, 2.2 Hz), Me-26 ($\delta$ 1.23, s), Me-27 ($\delta$ 1.23, s); $^{13}C$ NMR ($CD_3OD$, 150 MHz) data of aglycon moiety superimposable on those reported for compound **1**, excepted for C-24 ($\delta$ 78.9), C-25 ($\delta$ 80.9), Me-26 ($\delta$ 21.0), Me-27 ($\delta$ 23.3); $^1H$ NMR ($CD_3OD$, 600 MHz) and $^{13}C$ NMR ($CD_3OD$, 150 MHz) data of sugar portion, see Table 1; ESIMS *m/z* 981 $[M+Na]^+$; ESIMS/MS *m/z* 921 $[M+Na-60]^+$, 789 $[M+Na-60-132]^+$, 775 $[M+Na-60-146]^+$; HRMALDITOFMS *m/z* 981.5401 $[M+Na]^+$ (calcd for $C_{49}H_{82}O_{18}Na$, 981.5399).

#### 4.3.3. Eremophiloside C (*3*)

White amorphous powder; mp 278–280 °C; $[\alpha]_D^{25}$ +23.7 (*c* 0.2, MeOH); IR (KBr) $\nu_{max}$ 3393, 2926, 1265–1056 $cm^{-1}$; $^1H$ NMR ($CD_3OD$, 600 MHz) data of aglycon moiety, see Table 2; $^{13}C$ NMR ($CD_3OD$, 150 MHz) data of aglycon moiety, see Table 5; $^1H$ NMR ($CD_3OD$, 600 MHz) and $^{13}C$ NMR ($CD_3OD$, 150 MHz) data of sugar portion, see Table 1; ESIMS *m/z* 795 $[M+Na]^+$; ESIMS/MS *m/z* 663 $[M+Na-132]^+$, 513 $[M+Na-132-132]^+$, 305 $[M+Na-490]^+$; HRMALDITOFMS *m/z* 795.4504 $[M+Na]^+$ (calcd for $C_{40}H_{68}O_{14}Na$, 795.4507).

#### 4.3.4. Eremophiloside D (**4**)

White amorphous powder; mp 289–291 °C; $[\alpha]_D^{25}$ +10.3 (*c* 0.1, MeOH); IR (KBr) $\nu_{max}$ 3425, 2922, 1734, 1258–1045 $cm^{-1}$; $^1H$ NMR ($CD_3OD$, 600 MHz) data of aglycon moiety, see Table 2; $^{13}C$ NMR ($CD_3OD$, 150 MHz) data of aglycon moiety, see Table 5; $^1H$ NMR ($CD_3OD$, 600 MHz) and $^{13}C$ NMR ($CD_3OD$, 150 MHz) data of sugar portion, see Table 1; ESIMS *m/z* 793 $[M+Na]^+$; ESIMS/MS *m/z* 661 $[M+Na-132]^+$, 511 $[M+Na-132-132]^+$, 305 $[M+Na-488]^+$; HRMALDITOFMS *m/z* 793.4354 $[M+Na]^+$ (calcd for $C_{40}H_{66}O_{14}Na$, 793.4350).

#### 4.3.5. Eremophiloside E (**5**)

White amorphous powder; mp 275–278 °C; $[\alpha]_D^{25}$ −9.9 (*c* 0.15, MeOH); IR (KBr) $\nu_{max}$ 3448, 2950, 1740, 1235–1044 $cm^{-1}$; $^1H$ NMR ($CD_3OD$, 600 MHz) data of aglycon moiety, see Table 3; $^{13}C$ NMR ($CD_3OD$, 150 MHz) data of aglycon moiety, see Table 5; $^1H$ NMR ($CD_3OD$, 600 MHz) and $^{13}C$ NMR ($CD_3OD$, 150 MHz) data of sugar portion, see Table 1; ESIMS *m/z* 703 $[M+Na]^+$; ESIMS/MS *m/z* 571 $[M+Na-132]^+$, 439 $[M+Na-132-132]^+$, 305 $[M+Na-398]^+$; HRMALDITOFMS *m/z* 703.3665 $[M+Na]^+$ (calcd for $C_{36}H_{56}O_{12}Na$, 703.3669).

#### 4.3.6. Eremophiloside F (**6**)

White amorphous powder; mp 285–288 °C; $[\alpha]_D^{25}$ +11.1 (*c* 0.1, MeOH); IR (KBr) $\nu_{max}$ 3482, 2940, 1740, 1693, 1283–1037 $cm^{-1}$; $^1H$ NMR ($CD_3OD$, 600 MHz) data of aglycon moiety, see Table 3; $^{13}C$ NMR ($CD_3OD$, 150 MHz) data of aglycon moiety, see Table 5; $^1H$ NMR ($CD_3OD$, 600 MHz) and $^{13}C$ NMR ($CD_3OD$, 150 MHz) data of sugar portion, see Table 1; ESIMS *m/z* 701 $[M+Na]^+$; ESIMS/MS *m/z* 569 $[M+Na-132]^+$, 437 $[M+Na-132-132]^+$, 305 $[M+Na-305]^+$; HRMALDITOFMS *m/z* 701.3518 $[M+Na]^+$ (calcd for $C_{36}H_{54}O_{12}Na$, 701.3513).

#### 4.3.7. Eremophiloside G (**7**)

White amorphous powder; mp 160–162 °C; $[\alpha]_D^{25}$ −30.8 (*c* 0.1, MeOH); IR (KBr) $\nu_{max}$ 3448, 2936, 1740, 1636, 1268–1068 $cm^{-1}$; $^1H$ NMR ($CD_3OD$, 600 MHz) data of aglycon moiety, see Table 3; $^{13}C$ NMR ($CD_3OD$, 150 MHz) data of aglycon moiety, see Table 5; $^1H$ NMR ($CD_3OD$, 600 MHz) and $^{13}C$ NMR ($CD_3OD$, 150 MHz) data of sugar portion, see Table 1; ESIMS *m/z* 757 $[M+Na]^+$; ESIMS/MS *m/z* 625 $[M+Na-132]^+$, 493 $[M+Na-132-132]^+$, 305 $[M+Na-452]^+$; HRMALDITOFMS *m/z* 757.4132 $[M+Na]^+$ (calcd for $C_{40}H_{62}O_{12}Na$, 757.4139).

#### 4.3.8. Eremophiloside H (**8**)

White amorphous powder; mp 169–171 °C; $[\alpha]_D^{25}$ −10.7 (*c* 0.1, MeOH); IR (KBr) $\nu_{max}$ 3411, 2952, 1740, 1275–1023 $cm^{-1}$; $^1H$ NMR ($CD_3OD$, 600 MHz) data of aglycon moiety, see Table 4; $^{13}C$ NMR ($CD_3OD$, 150 MHz) data of aglycon moiety, see Table 5; $^1H$ NMR ($CD_3OD$, 600 MHz) and $^{13}C$ NMR ($CD_3OD$, 150 MHz) data of sugar portion, see Table 1; ESIMS *m/z* 789 $[M+Na]^+$; ESIMS/MS *m/z* 657 $[M+Na-132]^+$, 525 $[M+Na-132-132]^+$, 305 $[M+Na-484]^+$; HRMALDITOFMS *m/z* 789.4407 $[M+Na]^+$ (calcd for $C_{41}H_{66}O_{13}Na$, 789.4401).

#### 4.3.9. Eremophiloside I (**9**)

White amorphous powder; mp 170–173 °C; $[\alpha]_D^{25}$ −12.0 (*c* 0.1, MeOH); IR (KBr) $\nu_{max}$ 3448, 2954, 1740, 1266–1044 $cm^{-1}$; $^1H$ NMR ($CD_3OD$, 600 MHz) data of aglycon moiety, see Table 4; $^{13}C$ NMR ($CD_3OD$, 150 MHz) data of aglycon moiety, see Table 5; $^1H$ NMR ($CD_3OD$, 600 MHz) and $^{13}C$ NMR ($CD_3OD$, 150 MHz) data of sugar portion, see Table 1; ESIMS *m/z* 803 $[M+Na]^+$; ESIMS/MS *m/z* 671 $[M+Na-132]^+$, 539 $[M+Na-132-132]^+$, 305 $[M+Na-498]^+$; HRMALDITOFMS *m/z* 803.4563 $[M+Na]^+$ (calcd for $C_{42}H_{68}O_{13}Na$, 803.4558).

#### 4.3.10. Eremophiloside J (**10**)

White amorphous powder; mp 260–262 °C; $[\alpha]_D^{25}$ +13.9 (*c* 0.1, MeOH); IR (KBr) $\nu_{max}$ 3430, 2958, 1268–1039 $cm^{-1}$; $^1H$ NMR ($CD_3OD$, 600 MHz) data of aglycon moiety, see Table 4; $^{13}C$ NMR ($CD_3OD$, 150 MHz) data of aglycon moiety, see Table 5; $^1H$ NMR ($CD_3OD$, 600 MHz) and $^{13}C$ NMR ($CD_3OD$, 150 MHz) data of sugar portion, see Table 1; ESIMS *m/z* 791 $[M+Na]^+$; ESIMS/MS *m/z* 659 $[M+Na-132]^+$, 527 $[M+Na-132-132]^+$, 305 $[M+Na-486]^+$; HRMALDITOFMS *m/z* 791.4199 $[M+Na]^+$ (calcd for $C_{40}H_{64}O_{14}Na$, 791.4194).

#### 4.3.11. Eremophiloside K (**11**)

White amorphous powder; mp 269–271 °C; $[\alpha]_D^{25}$ +7.5 (*c* 0.1, MeOH); IR (KBr) $\nu_{max}$ 3417, 2949, 1740, 1255–1063 $cm^{-1}$; $^1H$ NMR ($CD_3OD$, 600 MHz) data of aglycon moiety, see Table 4; $^{13}C$ NMR ($CD_3OD$, 150 MHz) data of aglycon moiety, see Table 5; $^1H$ NMR ($CD_3OD$, 600 MHz) and $^{13}C$ NMR ($CD_3OD$, 150 MHz) data of sugar portion, see Table 1; ESIMS *m/z* 789 $[M+Na]^+$; ESIMS/MS *m/z* 657 $[M+Na-132]^+$, 525 $[M+Na-132-132]^+$, 305 $[M+Na-484]^+$; HRMALDITOFMS *m/z* 789.4043 $[M+Na]^+$ (calcd for $C_{40}H_{62}O_{14}Na$, 789.4037).

### 4.4. Biological assays

#### 4.4.1. Reagents

Fetal bovine serum (FBS) was from Bio-Whittaker. All the other chemicals were purchased from Sigma–Aldrich (MO, USA).

#### 4.4.2. Cell culture

Breast cancer MCF7 cells were maintained in DMEM medium supplemented with 10% (v/v) fetal bovine serum (FBS), 2 mM L-glutamine, and antibiotics (100 U/mL penicillin, 100 μg/mL streptomycin) at 37 °C in humidified atmosphere with 5% $CO_2$. Leukocyte cancer U937 cells were grown in RPMI 1640 medium at the same conditions described above. To ensure logarithmic growth, cells were sub-cultured every 2 days.

#### 4.4.3. Cell number evaluation

U937 and MCF7 cells were seeded in 96-well plates at a cell density of $2\times10^4$/well and $1\times10^4$/well, respectively, and exposed to increasing concentrations (1–50 μM) of compounds **1**–**11** or of the vehicle only (DMSO, less than 0.2% final concentration) up to 48 h. Then, the number of cells was quantified by using the Promega's CellTiter-Blue® Cell Viability assay. The CellTiter-Blue® reagent was added and the cultures incubated for 1 h before fluorescence readings were taken. To exclude any interference of test compounds with the viability assay we monitored in preliminary experiments the absence of fluorescence of pure compounds (dissolved in the cell medium) at the wavelengths used in the test.

#### 4.4.4. Cytofluorimetric analysis

The effect of test compounds on cell viability and on cell cycle progression was evaluated in U937 cells exposed to the drugs for 24 h.

Necrosis was quantified by propidium iodide (PI) staining of non-permeabilized cells.[32] Control and treated cells were collected, washed twice with phosphate buffered saline (PBS), resuspended at a density of $2\times10^5$ cells/mL in 4 μg/mL PI/PBS solution, and then immediately analyzed by flow cytometry (FACScalibur, Becton Dickinson, San Jose, CA, USA). Data from 10,000 events per sample were collected and analyzed using CellQuest software.

Apoptosis was evaluated by PI incorporation in permeabilized cells.[33] Control and treated cells were collected, washed twice with PBS, and then resuspended ($2\times10^5$ cells/mL) in PI hypotonic solution (0.1% sodium citrate, 0.1% Triton X-100, 50 μg/mL PI). Following incubation at 4 °C for 30 min in the dark, the DNA content of cell nuclei was measured by flow cytometry. Data from 10,000 events

per sample were collected and the percentage of the elements in the hypodiploid region was calculated using the CellQuest software. In each experiment cells treated with 25 μM etoposide, a cytoreductive agent known to induce apoptosis in human hematopoietic cells, was included as positive control.

To evaluate cell cycle distribution, cells treated with test compound for 24 h and control were harvested and nuclei were labeled with PI as described for apoptosis detection and analyzed by flow cytometry. Data from 20,000 events per sample were collected and the relative percentages of the cells in $G_0/G_1$, S and $G_2/M$ phases of the cell cycle were determined using the MODFIT software (Becton Dickinson, San Jose, CA, USA).

*4.4.5. Data analysis*

Data are expressed as the mean±S.D. of at least two independent experiments, performed in duplicate, showing similar results. Data were analyzed by one-way ANOVA and considered significant when $^{*}P<0.05$, $^{**}P<0.01$.

## References and notes


1. *Trease and Evans Pharmacognosy*, 14th ed.; Evans, W. C., Ed.; W.B. Saunders: Philadelphia, PA, 1998; p 40.
2. Boulos, L.; *Flora of Egypt*, 1st ed.; Alhadara: Cairo, Egypt, 1999; Vol. 1, pp 320–336.
3. Tang, W. *Chinese Drugs of Plant Origin*; Springer: Berlin, 1992, pp 191–197.
4. Rios, L. J.; Waterman, P. G. *Phytother. Res.* **1997**, *11*, 411–418.
5. Verotta, L.; El-Sebakhy, N. A. *Studies in Natural Products Chemistry: Bioactive Natural Products*; Elsevier: Amsterdam, 2001; Vol. 25, Part F, pp 179–234.
6. Isaev, M. I.; Gorovits, M. B.; Abubakirov, N. K. *Chem. Nat. Compd.* **1989**, *25*, 131–147.
7. Çaliş, İ.; Yuruker, A.; Tasdemir, D.; Wright, A. D.; Sticher, O.; Luo, Y.-D.; Pezzuto, J. M. *Planta Med.* **1997**, *63*, 183–186.
8. Bedir, E.; Pugh, M.; Çaliş, İ.; Pasco, D. S.; Khan, I. A. *Biol. Pharm. Bull.* **2000**, *23*, 834–837.
9. Yesilada, E.; Bedir, E.; Çaliş, İ.; Takaishi, Y.; Ohmoto, Y. *J. Ethnopharmacol.* **2005**, *96*, 71–77.
10. Özipek, M.; Dönmez, A. A.; Çaliş, İ.; Brun, R.; Rüedi, P.; Tasdemir, D. *Phytochemistry* **2005**, *66*, 1168–1173.
11. Radwan, M. M.; El-Sebakhy, N. A.; Asaad, A. M.; Toaima, S. M.; Kingston, D. G. I. *Phytochemistry* **2004**, *65*, 2909–2913.
12. Radwan, M. M.; Farooq, A.; El-Sebakhy, N. A.; Asaad, A. M.; Toaima, S. M.; Kingston, D. G. I. *J. Nat. Prod.* **2004**, *67*, 487–490.
13. Verotta, L.; Orsini, F.; Tato, M.; El-Sebakhy, N. A.; Toaima, S. M. *Phytochemistry* **1998**, *49*, 845–852.
14. Verotta, L.; Tato, M.; El-Sebakhy, N. A.; Toaima, S. M. *Phytochemistry* **1998**, *48*, 1403–1409.
15. Verotta, L.; Guerrini, M.; El-Sebakhy, N. A.; Asaad, A. M.; Toaima, S. M.; Abou-Sheer, M. E.; Luo, Y. D.; Pezzuto, J. M. *Fitoterapia* **2001**, *72*, 894–905.
16. Verotta, L.; Guerrini, M.; El-Sebakhy, N. A.; Asaad, A. M.; Toaima, S. M.; Abou-Sheer, M. E.; Luo, Y. D.; Pezzuto, J. M. *Planta Med.* **2002**, *68*, 986–994.
17. El-Sebakhy, N. A.; Harraz, F. M.; Abdallah, R. M.; Asaad, A. M.; Orsini, F.; Sello, G.; Verotta, L. *Phytochemistry* **1990**, *29*, 3271–3274.
18. Abdallah, R. M.; Ghazy, N. M.; El-Sebakhy, N. A.; Pirillo, A.; Verotta, L. *Pharmazie* **1993**, *48*, 452–454.
19. Abdallah, R. M.; Ghazy, N. M.; Asaad, A. M.; El-Sebakhy, N. A.; Pirillo, A.; Verotta, L. *Pharmazie* **1994**, *49*, 377–378.
20. Gariboldi, P.; Pelizzoni, F.; Tato, M.; Verotta, L.; El-Sebakhy, N.; Asaad, A. M.; Abdallah, R. M.; Toaima, S. M. *Phytochemistry* **1995**, *40*, 1755–1760.
21. Kikuchi, T.; Akihisa, T.; Tokuda, H.; Ukiya, M.; Watanabe, K.; Nishino, H. *J. Nat. Prod.* **2007**, *70*, 918–922.
22. Tian, Z.; Yang, M.; Huang, F.; Li, K.; Si, J.; Shi, L.; Chen, S.; Xiao, P. *Cancer Lett.* **2005**, *226*, 65–75.
23. Isaev, M. I.; Gorovits, M. B.; Abdullaev, N. D.; Abubakirov, N. K. *Chem. Nat. Compd.* **1983**, *18*, 424–430.
24. Kaipnazarov, T. N.; Uteniyazov, K. K.; Saatov, Z. *Chem. Nat. Compd.* **2004**, *40*, 40–44.
25. Mamedova, R. P.; Agzamova, M. A.; Turgunov, K. K.; Tozhiboev, A.; Tashkhodzhaev, B.; Isaev, M. I. *Chem. Nat. Compd.* **2006**, *42*, 501–502.
26. Matsumori, N.; Kaneno, D.; Murata, M.; Nakamura, H.; Tachibana, K. *J. Org. Chem.* **1999**, *64*, 866–876.
27. Mamedova, R. P.; Agzamova, M. A.; Isaev, M. I. *Chem. Nat. Compd.* **2003**, *39*, 470–474.
28. Liu, Y.; Chen, D.; Si, J.; Tu, G.; An, D. *J. Nat. Prod.* **2002**, *65*, 1486–1488.
29. Gao, J.; Huang, F.; Zhang, J.; Zhu, G.; Yang, M.; Xiao, P. *J. Nat. Prod.* **2006**, *69*, 1500–1502.
30. Kusano, A.; Takahira, M.; Shibano, M.; Miyase, T.; Okuyama, T.; Kusano, G. *Heterocycles* **1998**, *48*, 1003–1013.
31. Uhrín, D.; Batta, G.; Hruby, V. J.; Barlow, P. N.; Kövér, K. E. *J. Magn. Reson.* **1998**, *130*, 155–161.
32. Bedner, E.; Li, X.; Gorczyca, W.; Melamed, M. R.; Darzynkiewicz, Z. *Cytometry* **1999**, *35*, 181–195.
33. Nicoletti, I.; Migliorati, G.; Pagliacci, M. C.; Grignani, F.; Riccardi, C. *J. Immunol. Methods* **1991**, *139*, 271–279.